Am J Physiol Heart Circ Physiol 315: H512–H521, 2018.
First published May 18, 2018; doi:10.1152/ajpheart.00160.2018.

RESEARCH ARTICLE | *Signaling and Stress Response*

Transactivation domain of p53 regulates DNA repair and integrity in human iPS cells

Ramaswamy Kannappan, Saidulu Mattapally, Pooja A. Wagle, and Jianyi Zhang

Department of Biomedical Engineering, School of Medicine, School of Engineering, The University of Alabama at Birmingham, Birmingham, Alabama

Submitted 27 February 2018; accepted in final form 3 May 2018

Kannappan R, Mattapally S, Wagle PA, Zhang J. Transactivation domain of p53 regulates DNA repair and integrity in human iPS cells. *Am J Physiol Heart Circ Physiol* 315: H512–H521, 2018. First published May 18, 2018; doi:10.1152/ajpheart.00160.2018.—The role of p53 transactivation domain (p53-TAD), a multifunctional and dynamic domain, on DNA repair and retaining DNA integrity in human induced pluripotent stem cells (hiPSCs) has never been studied. p53-TAD was knocked out in iPSCs using CRISPR/Cas9 and was confirmed by DNA sequencing. p53-TAD knockout (KO) cells were characterized by accelerated proliferation, decreased population doubling time, and unaltered Bcl-2, Bcl-2-binding component 3, insulin-like growth factor 1 receptor, and Bax and altered Mdm2, p21, and p53-induced death domain transcript expression. In p53-TAD KO cells, the p53-regulated DNA repair proteins xeroderma pigmentosum group A, DNA polymerase H, and DNA-binding protein 2 expression were found to be reduced compared with p53 wild-type cells. Exposure to a low dose of doxorubicin (Doxo) induced similar DNA damage and DNA damage response (DDR) as measured by RAD50 and MRE11 expression, checkpoint kinase 2 activation, and γH2A.X recruitment at DNA strand breaks in both cell groups, indicating that silence of p53-TAD does not affect the DDR mechanism upstream of p53. After removal of Doxo, p53 wild-type hiPSCs underwent DNA repair, corrected their damaged DNA, and restored DNA integrity. Conversely, p53-TAD KO hiPSCs did not undergo complete DNA repair and failed to restore DNA integrity. More importantly, continuous culture of p53-TAD KO hiPSCs underwent G_2/M cell cycle arrest and expressed the cellular senescent marker $p16^{INK4a}$. Our data clearly show that silence of the TAD of p53 did not affect DDR but affected the DNA repair process, implying the crucial role of p53-TAD in maintaining DNA integrity. Therefore, activating p53-TAD domain using small molecules may promote DNA repair and integrity of cells and prevent cellular senescence.

NEW & NOTEWORTHY The p53 transactivation domain (TAD) in human induced pluripotent stem cells (iPSCs) was deleted using the CRISPR/Cas9 system. Deletion of p53-TAD resulted in increased cell proliferation but did not affect iPSC pluripotency. DNA repair machinery upstream of p53 was not affected in p53-TAD knockout, but p53-regulated DNA repair proteins xeroderma pigmentosum group A, DNA polymerase H, and DNA-binding protein 2 were affected. Finally, p53-TAD was found to be necessary for iPSCs to repair damaged DNA and retain DNA integrity.

cellular senescence; DNA repair; human induced pluripotent stem cells; p53

INTRODUCTION

The possibility of inducing pluripotency in somatic cells and even further generating cardiomyocyte from induced pluripotent stem cells (iPSCs) through forced expression of reprogramming factors has opened new attractive options for cardiovascular regenerative medicine (24). The storehouse of genetic data in every living cell, including iPSCs, is DNA; therefore, its integrity is fundamental to life. However, DNA is not inert. Metabolic compounds in the cell, such as reactive oxygen, carbonyl and nitrogen species, and alkylating agents, can damage DNA (13, 20, 30, 31). These injuries occur instinctively in every cell, and the rate of incidence is significant. Unrepaired damage leads to mutation, DNA instability, cellular senescence, and possibly diseases, including life-threatening cancers. Retaining DNA integrity is essential to any cell, especially human iPSCs, which possess immense clinical potential. In fact, every cell has numerous tools to detect and repair different types of DNA impairment. The major transcription factor p53 regulates a wide range of cellular processes, including cell death and cell cycle progression, cell metabolism, autophagy, mRNA translation feedback mechanisms, and, most importantly, DNA damage repair for maintaining DNA integrity (23, 27, 34).

p53 protein contains four functional domains: a transcriptional activation domain (TAD), a DNA-binding domain, a tetramerization domain, and a COOH-terminal basic domain (12). Each domain performs an integral role in enabling the various functions of p53. The DNA-binding domain is responsible for the fundamental role of the p53 family of proteins, as a sequence-specific transcription factor (12). The tetramerization domain enables p53 to undergo tetramerization, which is essential for its high DNA binding affinity and transcriptional activation (3). The COOH-terminal basic domain, which serves as a regulatory domain, can both positively and negatively regulate p53 activities (11). The NH_2-terminus TAD of p53, which is the focus of this report, is crucial for the function of the p53 family of proteins.

The NMR spectroscopy structure of p53 has revealed that the unstructured and natively unfolded p53-TAD is composed of two TADs: TAD1 and TAD2 (Fig. 1*A*) (6). Deletion and mutation of p53-TAD1 indicates that TAD1 is unnecessary for apoptosis but is a prerequisite for cell cycle arrest (26). Particularly, inducible expression of p53 carrying the TAD1 mutation resulted in cell death without significant cell cycle arrest (36), whereas p53-TAD2 mutants were unable to induce apoptosis but retain a modest ability to undergo cell cycle arrest (35). Similarly, an apoptotic defect was also found in a mouse with deletion of p53

Address for reprint requests and other correspondence: R. Kannappan, Univ. of Alabama at Birmingham, 1670 University Blvd., VH G094S, Birmingham, AL 35233 (e-mail: ramkn@uab.edu).

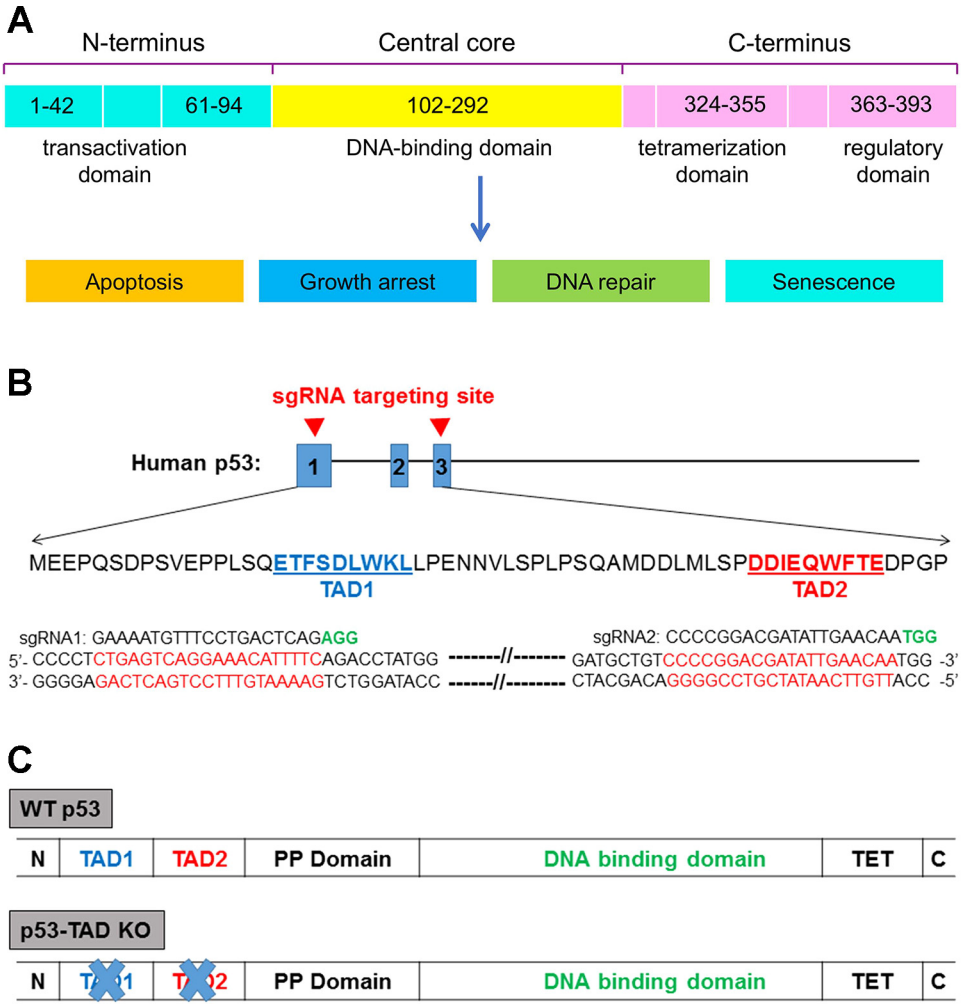

Fig. 1. p53 transactivation domain (TAD) knockout (KO) scheme. *A*: human p53 protein structure domains and functions. *B* and *C*: schematic of CRISPR/Cas9 knockout of p53-TADs in human induced pluripotent stem cells (hiPSCs). sgRNA, single-guide RNA; N, NH_2-terminal; C, COOH-terminal; WT, wild-type.

proline-rich residues (9). p53 plays a prominent role as a facilitator of DNA repair by halting the cell cycle to allow time for the repair machineries to restore genome stability. However, whether p53-TAD has any direct role on DNA repair processes is yet to be unraveled. Therefore, in this study, we aimed to determine if p53-TAD is involved in DNA repair and integrity in human cardiac fibroblast-derived iPSCs. Ideally, it would be reasonable to study the role of p53-TAD in the DNA repair process by knocking out p53-TAD1 and p53-TAD2 separately. Considering the association of p53-TAD1 with the induction of apoptosis (36), activation of p53 by inducing DNA damage in p53-TAD1 knockout (KO) cells would result in cell death. As cell survival is important to study, and because the DNA repair mechanism and role of p53-TAD1 have already been established (36), it is logical to delete both p53-TADs from the cells. To achieve this, we knocked out both TAD1 and TAD2 of p53 in human (h)iPSCs using CRISPR/Cas9 gene KO technology, and here we report our findings.

MATERIALS AND METHODS

p53-TAD-deficient stable cell line using CRISPR/Cas9. Plasmid pLentiCRISPR V2 was a gift from Feng Zhang (Addgene plasmid no. 52961). Two guide sequences [single guide (sg)RNA1: 5′-GAAAATGTTTCCTGACTCAG-3′ and sgRNA2: 5′-CCCCGGACGATATTGAACAA-3′] for human Tp53 (NCBI Accession No. NM_000546.5) flanking the TADs were designed using the online program (http://crispr.mit.edu/). Two oligos for each guide sequences were then synthesized (Invitrogen) as follows: sgRNA1 oligos, forward 5′-CACCGGAAAATGTTTCCTGACTCAG-3′ and reverse 5′-AAACCTGAGTCAGGAAACATTTTCC-3′; and sgRNA2 oligos, forward 5′-CACCGCCCCGGACGATATTGAACAA-3′ and reverse 5′-AAACTTGTTCAATATCGTCCGGGGC-3′.

pLentiCRISPR V2 was digested by BsmBI, and the annealed oligos were then cloned into the vector. To make the lentivirus, pLentiCRISPR (with cloned sgRNA) was cotransfected with packaging plasmids pVSVg (no. 8454, AddGene), pRSV-Rev (no. 12253, AddGene), and pMDLg/pRRE (no. 12251, AddGene) into human embryonic kidney (HEK)-293(F) T cells. Packaged lentiviruses were collected from the supernatant. hiPSCs were then transduced with lentiviruses carrying CRISPR sgRNA targeting p53-TAD following the manufacturer's instructions. Transduced hiPSCs were selected in growth medium containing 5 μg/ml puromycin (P8833, Sigma) for 48 h. Cells were seeded sparsely and cultured normally to get visible individual clones. These clones were picked and propagated. Clones were screened for p53-TAD KO by Sanger sequencing and confirmed by Western blot analysis.

iPSC culture. Previously generated and published human cardiac fibroblast-derived iPSCs were used in this study (33). hiPSCs were cultured in mTeSR1 medium (Stemcell Technologies) using our previously published methods (33).

Population doubling time and Western blot analysis. Human iPSCs were plated at low density. The number of cells per unit area was determined at the time of seeding and 24 h later. Population doubling

time was computed by linear regression of $\log_2$ values of cell numbers. Protein lysates of hiPSCs were obtained using RIPA buffer (Sigma-Aldrich) and protease inhibitors. Equivalents of 10 μg proteins were separated using 4–20% SDS-PAGE and subjected to Western blot analysis. The following antibodies were used: NH_2-terminal-specific rabbit monoclonal anti-p53 (Cell Signaling Technology, Danvers, MA), rabbit COOH-terminal anti-p53 (Sigma-Aldrich), rabbit monoclonal anti-checkpoint kinase 2 (Chk2; Thr^{68}, Cell Signaling Technology), rabbit monoclonal anti-Chk2 (Cell Signaling Technology), rabbit monoclonal anti-Mre11 (Cell Signaling Technology), rabbit anti-Rad50 (Cell Signaling Technology), rabbit anti-xeroderma pigmentosum group D (XPD; D3Z6I, Cell Signaling Technology), rabbit anti-xeroderma pigmentosum group A (XPA; D9U5U, Cell Signaling Technology), rabbit anti-DNA polymerase H (DNA Pol η; E1I7T, Cell Signaling Technology), and rabbit anti-DNA-binding protein 2 (DDB2; D4C4, Cell Signaling Technology). Loading conditions were determined by GAPDH.

Proliferation, apoptosis, and senescence. The baseline condition of these cellular parameters was measured in hiPSCs with p53 wild-type (WT) and p53-TAD KO. For proliferation, cells were seeded in 96-well plates (3×10^3 cells/well) and cultured for 48 h. Dehydrogenase activity as a measurement of cell proliferation was measured with a MTS assay kit following the manufacturer's protocol (G1112, Promega). For apoptosis, cells were seeded in 96-well plates (3×10^3 cells/well) and cultured for 48 h. An apoptosis assay was performed using the Annexin V apoptosis detection kit (BDB556547, Fisher Scientific). For senescence, cells grown on Matrigel-coated coverslips were fixed in 4% paraformaldehyde, and the fraction of cells that reached replicative senescence and irreversible growth arrest was evaluated by the expression of the senescence-associated protein $p16^{INK4a}$ (Abcam).

DNA damage response and comet assay. For the DNA damage response, cells were grown on Matrigel-coated coverslips, fixed in 4% paraformaldehyde, and immunolabeled with a human anti-phosphohistone H2A.X (Ser^{139}, Cell Signaling Technology). A fraction of γH2A.X-positive cells was counted using ImageJ software (National Institutes of Health). The comet assay was performed using the OxiSelect Comet Assay kit (Cell Biolabs). Cells were embedded in agarose gel and placed on top of a microscope slide. Slides were treated with alkaline lysis buffer to remove proteins and subsequently immersed in Tris-EDTA buffer. Electrophoresis was performed to induce the formation of comets. Slides were stained with Vista green dye and analyzed by fluorescence microscopy (18). The distance between the center of the head and the center of the tail, i.e., the tail moment length, was measured with ImageJ using the comet assay plugin. The tail moment was then calculated by the product of the percentage of damaged DNA and the tail moment length.

Transcript analysis by RT-PCR. Total RNA was extracted from cells with TRIzol reagent (Invitrogen) and used to quantify transcripts of Oct4, Nanog, Sox2, and proliferation cell nuclear antigen (PCNA). cDNA for mRNAs was obtained from 2 μg total RNA in a 20-μl reaction using TaqMan Reverse Transcription Reagents (ThermoFisher Scientific) and 100 pmol of oligo$(dT)_{15}$ primer. This mixture was incubated at 37°C for 2 h. Quantitative RT-PCR was performed with the primers described below (see *RT-PCR primers*). The Eppendorf realplx^2 Real-Time PCR system was used. cDNA synthesized from 100 ng total RNA was combined with Maxima SYBR Green qPCR Master Mix (ThermoFisher Scientific) and 0.5 μM each of forward and reverse primers. Cycling conditions were as follows: 95°C for 10 min followed by 40 cycles of amplification (95°C denaturation for 15 s and 60°C annealing-extension for 1 min). To avoid the influence of genomic contamination, forward and reverse primers for each gene were located in different exons. Quantified values were normalized against the input determined by the housekeeping gene GAPDH.

RT-PCR primers. The following primers were used: human Oct4, forward 5′-CAGTGCCCGAAACCCACAC-3′ and 5′-GGAGACCCAGCAGCCTCAAA-3′; human Sox2, forward 5′-GTCATTTGCTGTGGGTGATG-3′ and reverse 5′-AGAAAAACGAGGGAAATGGG-3′; human Nanog, forward 5′-CAGAAGGCCTCAGCACCTAC-3′ and reverse 5′-ATTGTTCCAGGTCTGGTTGC-3′; human PCNA, forward 5′-TGTCGATAAAGAGGAGGAAGC-3′ and reverse 5′- AAGAGAGTGGAGTGGCTTTTG-3′; human MDM2, forward 5′-TGTTGTGAAAGAAGCAGTAGCA-3′ and reverse 5′-CCTGATCCAACCAATCACCT-3′; human cyclin-dependent kinase inhibitor 1A (CDKN1A), forward 5′-AGTCAGTTCCTTGTGGAGCC-3′ and reverse 5′-CATGGGTTCTGACGGACAT-3′; human p53-induced death domain protein, forward 5′-AAGGTTCCGTGGAGTCTGCT-3 and reverse 5′-CAGAGTGGTCAGGGTTCCAT-3′; human Bcl-2, forward 5′-CTGAGTACCTGAACCGGCA-3′ and reverse 5′-GAGAAATCAAACAGAGGCCG-3′; human Bax, forward 5′-CAGAGGCGGGGTTTCATC-3′ and reverse 5′-AGCTTCTTGGTGGACGCAT-3′; human insulin-like growth factor 1 receptor, forward 5′-GTACAACTACCGCTGCTGGA-3′ and reverse 5′-TGGCAGCACTCATTGTTCTC-3′; human Bcl-2-binding component 3 (BBC3), forward 5′-GTGTGGAGGAGGAGGAGTGG-3′ and reverse 5′-TGTCGATGCTGCTCTTCTTG-3′; human DNA-binding damage protein 2 (DDB2), forward 5′-ACCTCCGAGATTGTATTACGCC-3′ and reverse 5′-TCACATCTTCTGCTAGGACCG-3′; human XPD, forward 5′-GGAAGACAGTATCCCTGTTGGC-3′ and reverse 5′-CAATCTCTGGCACAGTTCTTGA-3′; human XPA, forward 5′-CCAGGACCTGTTATGGAATTTGA-3′ and reverse 5′-GCTTCTTGACTACCCCAAACTTC-3′; and human DNA Pol H, forward 5′-GCTACTGGACAGGATCGAGTG-3′ and reverse 5′-CACCACCCTTCCATGATTTGTA-3′.

Cell cycle analysis. Cells were collected, washed in PBS, and resuspended at 1×10^6 cells/ml in propidium iodide (PI) staining buffer (0.1% sodium citrate, 0.1% Triton X-100, and 20 μg/ml PI). Cells then were treated with 20 μg/ml RNase at room temperature for 30 min. Cell cycle histograms were generated after analysis of PI-stained cells by FACS with a BD FACSCalibur Analyzer. For each culture, at least 1×10^4 events were recorded. Histograms generated by FACS were analyzed by a Cell Cycle platform, FlowJo Software (version 10.4.1), to determine the percentage of cells in each phase (G_1, S, and G_2/M).

Data analysis. Data are presented as means ± SD. Statistical analysis was performed using SigmaStat v4.0 software. Data were initially tested for normality (Shapiro-Wilk test) and equal variance for assignment to parametric or nonparametric analysis. When the normality failed, the Mann-Whitney rank-sum test was performed. Comet assay parameters were also analyzed by one-way ANOVA followed by Kruskal-Wallis one-way ANOVA on ranks. $P < 0.05$ was considered significant.

RESULTS

CRISPR/Cas9, guide RNA design, and p53-TAD KO. To investigate the function of p53-TAD on DNA damage repair, using CRISPR/Cas9 gene KO technology, we knocked out p53-TAD in hiPSCs to generate a stable p53-TAD KO hiPSC line. Guide RNA sequences flanking TADs of human p53 (Fig. 1, *B* and *C*) were designed and cloned into pLentiCRISPR, and lentiviruses carrying p53-TAD sgRNA were produced as described above in METHODS. To establish a stable p53-TAD KO hiPSC line after puromycin selection, cells were sparsely seeded, and individual colonies were picked and propagated. Clones were screened for changes in the p53-TAD DNA sequences. Out of several clones, one clone had 16 nucleotide deletions at the TAD1 region and a single nucleotide addition at TAD2 (Fig. 2*A*). The nucleotide deletion at TAD1 introduced a new stop codon between TAD1 and TAD2, leading to a premature termination of translation. This may lead to a complete KO of p53; however, p53 RNA has several start

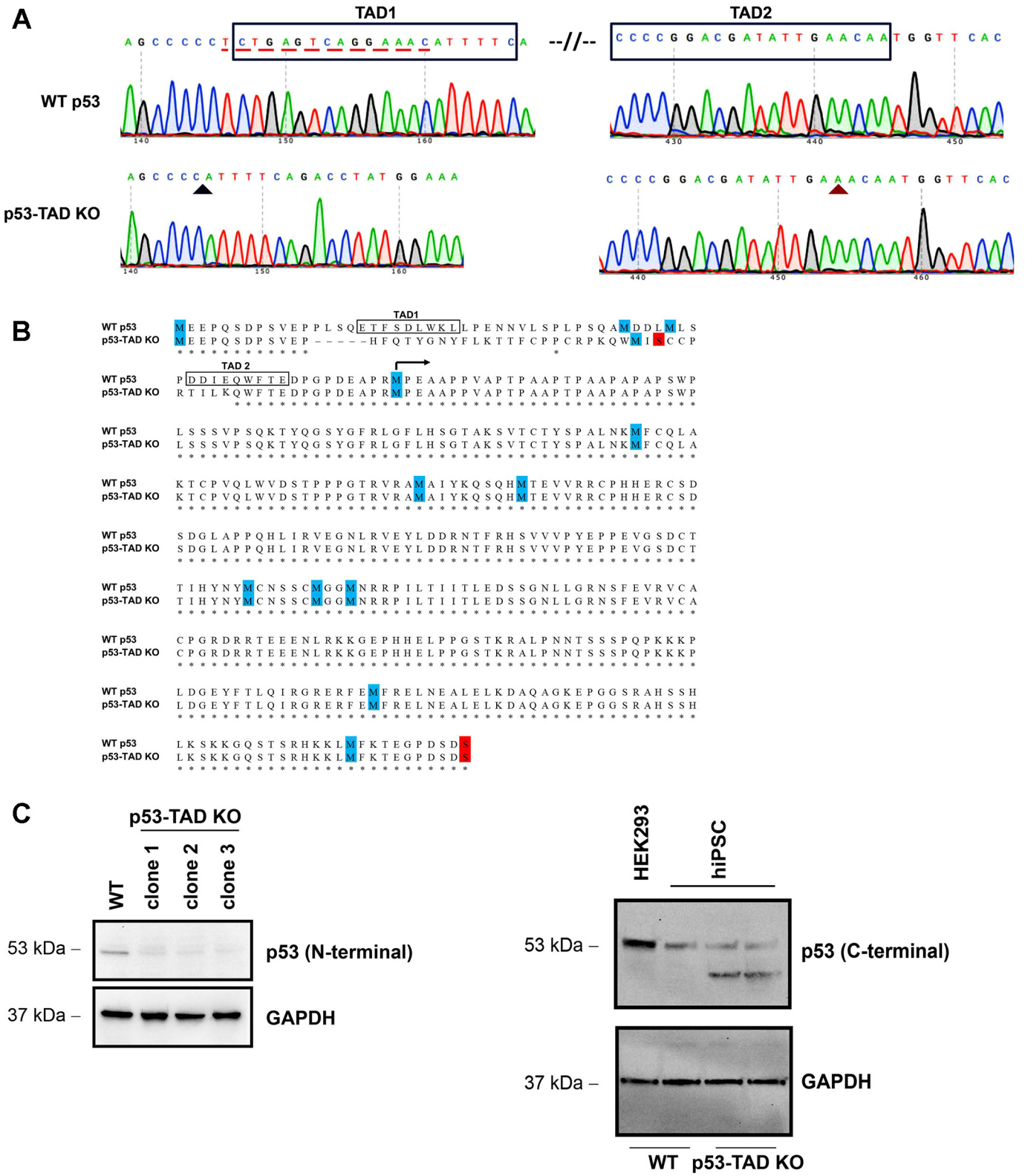

Fig. 2. p53 transactivation domain (TAD) knockout (KO). *A*: diagram showing the deletion of 11 bp (red dashed lines and black arrowhead) in p53 TAD1 (*bottom left*) and 1-bp addition (brown arrowhead) in TAD2 (*bottom right*). Box: single-guide (sg)RNA-binding site. *B*: amino acid sequence alignment of wild-type (WT) p53 and p53-TAD KO. Open boxes denote TAD1 and TAD2. Shaded blue boxes denote the translation starting site. Shaded red boxes denote the translation stop site. The bent arrow shows translation start site for truncated p53. *C*: Western blot analysis of p53 expression in puromycin-selected p53-TAD clones using antibody specific to NH_2-terminal (*left*) and COOH-terminal (*right*) domains of p53. HEK, human embryonic kidney; hiPSCs, human induced pluripotent stem cells.

codons, and the translation of RNA would resume from the next immediate start codon (Fig. 2*B* and Supplemental Fig. S1). The total protein lysate from these cells was subjected to Western blot analysis using an antibody specific for the p53 NH_2-terminal sequence. Three clones obtained out of several clones showed p53-TAD KO (Fig. 2*C*, *left*). Upon further analysis of these clones using a p53 COOH-terminal specific antibody, one of the clones, *clone 3*, revealed a 53-kDa band and an additional 47-kDa lower molecular weight band (Fig. 2*C*, *right*). The faint 53-kDa protein could be a p53 isoform. The lower 47-kDa band would be the truncated p53 protein. Collectively, DNA sequencing and Western blot analysis clearly indicated that TADs of p53 were knocked out in hiPSCs. *Clone 3* was cultured, expanded, and used for further experiments.

p53-TAD KO does not affect expression of hiPSC pluripotent markers. We analyzed whether the deletion of p53-TAD would damage the pluripotency of hiPSCs. p53-TAD KO iPSCs were immunolabeled for the pluripotent markers Nanog, Oct4, and Sox2 (Fig. 3*A*), and transcript expression of pluripotent markers were analyzed by quantitative real-time PCR (Fig. 3*B*). Expression of these pluripotent markers in p53-TAD KO cells were comparable to p53-WT hiPSCs.

Effect of p53-TAD KO on p53-regulated genes. Deletion of p53-TAD impairs the expression of p53-regulated genes. To characterize the p53-TAD KO cell, we analyzed the transcript expression of various p53-regulated genes by RT-PCR. Expression of MDM2, CDKN1A (p21), and p53-induced death domain were found to be downregulated; however, Bcl-2, Bax, insulin-like growth factor 1 receptor, and Puma (BBC3) transcript expression levels were not affected in p53-TAD hiPSCs compared with p53-WT hiPSCs (Fig. 3*C*). We also analyzed p53-regulated DNA repair genes, such as XPA, DDB2, DNA Pol η, and XPD. p53-TAD deletion in hiPSCs affected gene expression of XPA and DDB2 but not DNA Pol η and XPD (Fig. 3*D*). These data clearly conclude that the deletion of p53-TAD specifically affects certain gene expression but not all p53-regulated genes.

p53-TAD KO accelerates hiPSC proliferation. One of the critical roles of p53 is cell cycle regulation. Deletion of p53 in cells accelerates the growth of the cell in vitro and in vivo by promoting cell cycle progression (7, 8, 35). We tested whether p53-TAD deletion in hiPSCs would induce accelerated proliferation and mimic the effects of total p53 gene KO. Proliferation of WT and p53-TAD KO hiPSCs were measured by estimating NAD(P)H-dependent dehydrogenase enzyme activity using a MTS assay kit. Proliferation was 36% higher in TAD-p53 KO than WT hiPSCs (Fig. 4*A*), but no significant difference in cell death was observed (Fig. 4*B*). Because of increased proliferation, the average population doubling time reduced from 16.6 h (WT hiPSCs) to 10.7 h in TAD-p53 KO hiPSCs (Fig. 4*C*). However, the p53-regulated PCNA transcript did not show a significant change in expression (Fig. 4*D*). These data clearly show that because of the functional loss of p53 in p53-TAD KO, hiPSC cycle regulation was impaired, leading to increased proliferation and decreased population doubling time. Collectively, the proliferation, population doubling time, RT-PCR, and immunolabeling data show that p53-TAD deletion does not affect pluripotency of hiPSCs but accelerates cell cycle progression.

p53-TAD KO affects DNA damage repair. Next, we analyzed whether upstream of p53 in the DNA damage repair process is affected by p53-TAD deletion in hiPSCs. To induce DNA damage, doxorubicin (Doxo), a chemotherapeutic agent that is coupled with the formation of DNA strand breaks, was used. Both p53-WT and p53-TAD KO hiPSCs were exposed to the low dose of 0.25 μmol/l Doxo, and cell lysis was subjected to Western blot analysis. Expression of total Chk2 was comparable in both cell types. Chk2 underwent phosphorylation, a key mediator of DNA damage response (32), in both cell groups after Doxo treatment. However, levels of phosphorylated Chk2 were significantly higher in p53-TAD KO hiPSCs. Moreover, Rad50 and Mre11, the major components of the MRN complex that is recruited by the Chk2 at damaged DNA sites, were not found to be affected (Fig. 5*A*). Analysis of p53-regulated DNA repair proteins revealed that XPA, DNA Pol η, and DDB2 expression were significantly reduced at the basal level, whereas expression of XPD was not affected in p53-TAD KO hiPSCs. Interestingly, Doxo treatment had no effect on p53-regulaed DNA repair proteins in both p53-WT and p53-TAD KO hiPSCs except for XPA in WT cells (Fig. 5*B*). The γH2A.X protein accumulates at regions of DNA strand breaks, allowing the recognition of DNA damage (25, 28). Localization of γH2A.X at sites of DNA damage was present in Doxo-treated p53-TAD KO hiPS cells, indicating that assembly of γH2A.X is not affected by the deletion of p53-TAD (Fig. 5*C*). These data clearly show that activation and recruitment of DNA repair proteins were not affected by deletion of p53-TAD in hiPSCs.

To determine whether deletion of p53-TAD in hiPSCs affected DNA repair, both p53-WT and p53-TAD KO hiPSCs were treated with Doxo, and DNA damage was measured using a comet assay after 72 h of recovery (Fig. 5*D*). iPSCs were embedded in agarose on microscope slides and lysed to form nucleoids. After electrophoresis, slides were stained with Vista green dye, and comets were identified using fluorescence microscopy (Fig. 5*E*). The fluorescence intensity of the tail (damaged DNA) relative to the head (intact DNA) reflects the percentage of DNA damage. The distance between the center of the head and the center of the tail, i.e., the tail moment length, indicates the frequency of DNA strand breaks. Tail moment was calculated by the product of the percentage of damaged DNA and tail moment length. Tail moment provides a parameter that comprises both the extent of DNA damage and frequency of DNA strand breaks; this index was found to be comparable at baseline and to increase similarly in WT and

Fig. 3. p53 transactivation domain (TAD) deletion does not affect pluripotent markers in human induced pluripotent stem cells (hiPSCs). *A*: representative images of Oct4-, Sox2-, and Nanog-immunolabeled (red) p53-TAD knockout (KO) hiPSCs. Phalloidin is shown in green; the nucleus is shown in blue. *B*−*D*: mRNA transcript levels of pluripotent markers (*B*), p53-regulated genes (*C*), and p53-regulated DNA repair genes (*D*) in wild-type (WT) and p53-TAD KO hiPSCs as measured by RT-PCR. Symbols denote plotted values. Data are means ± SD; $n = 3$. *$P < 0.05$ vs. WT. RQ, relative quantity; a.u., arbitrary units; CDKN1A, cyclin-dependent kinase inhibitor 1A; PIDD, p53-induced death domain; XPA, xeroderma pigmentosum group A; DDB2, DNA-binding protein 2; IGF1R, insulin-like growth factor 1 receptor; DNA Pol η, DNA polymerase H; XPD, xeroderma pigmentosum group D; BBC3, Bcl-2-binding component 3.

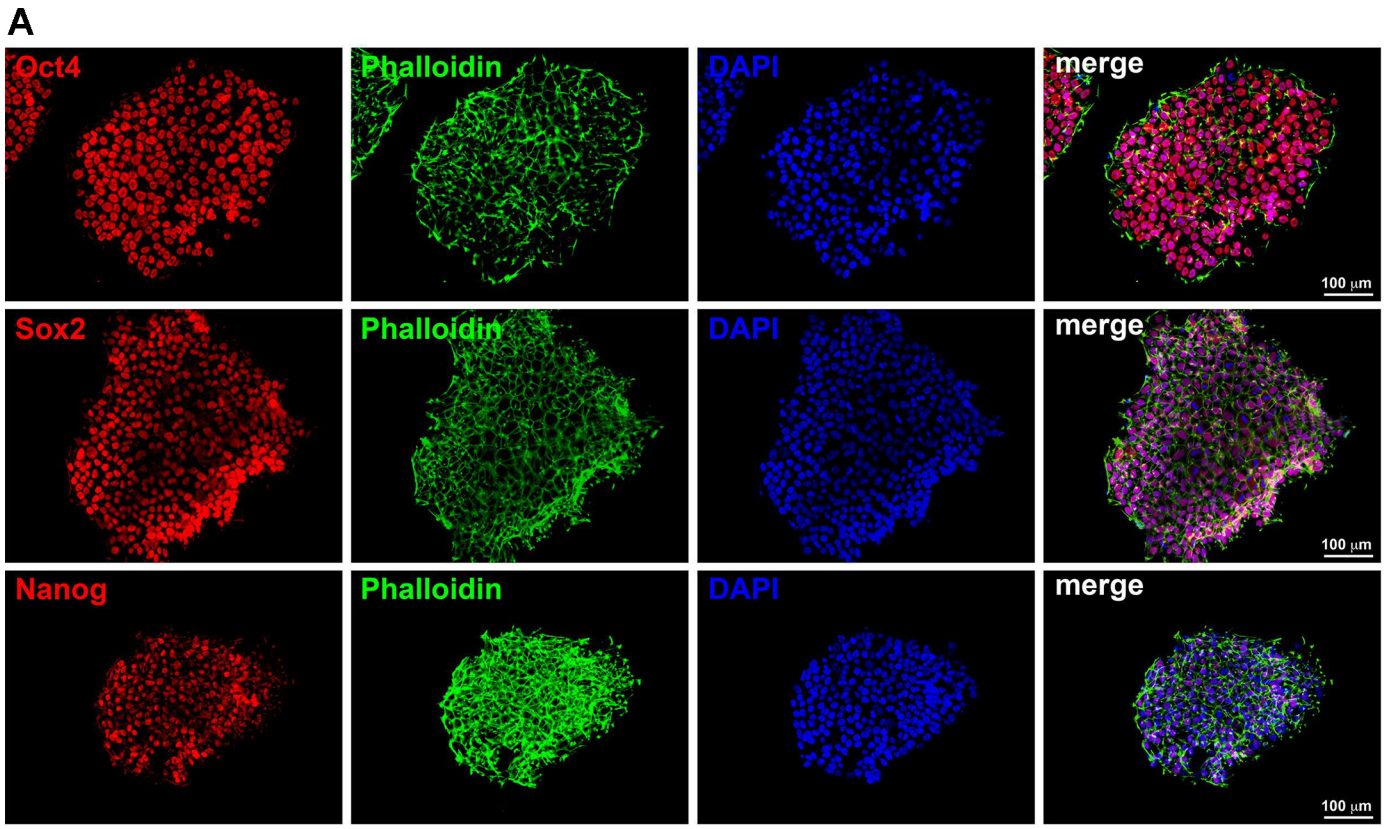

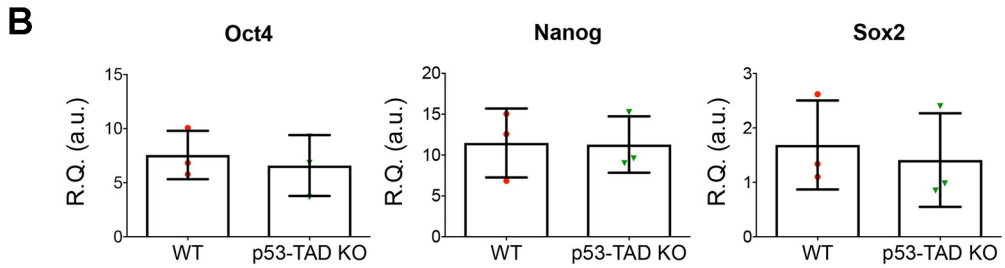

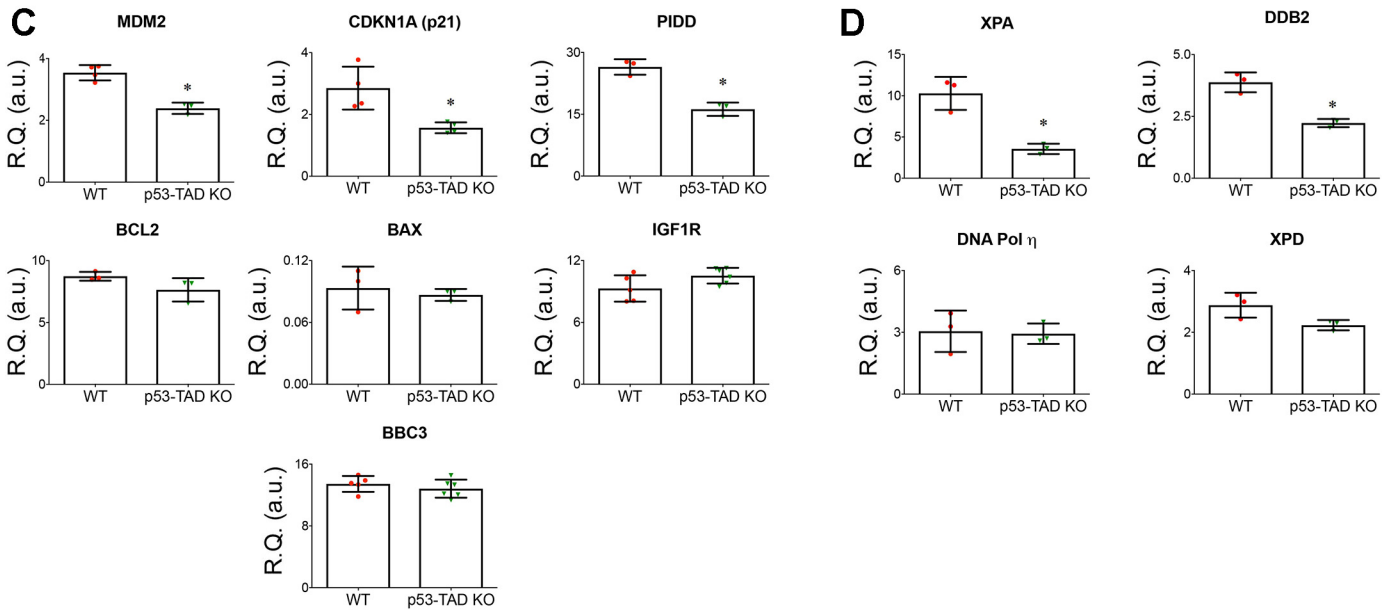

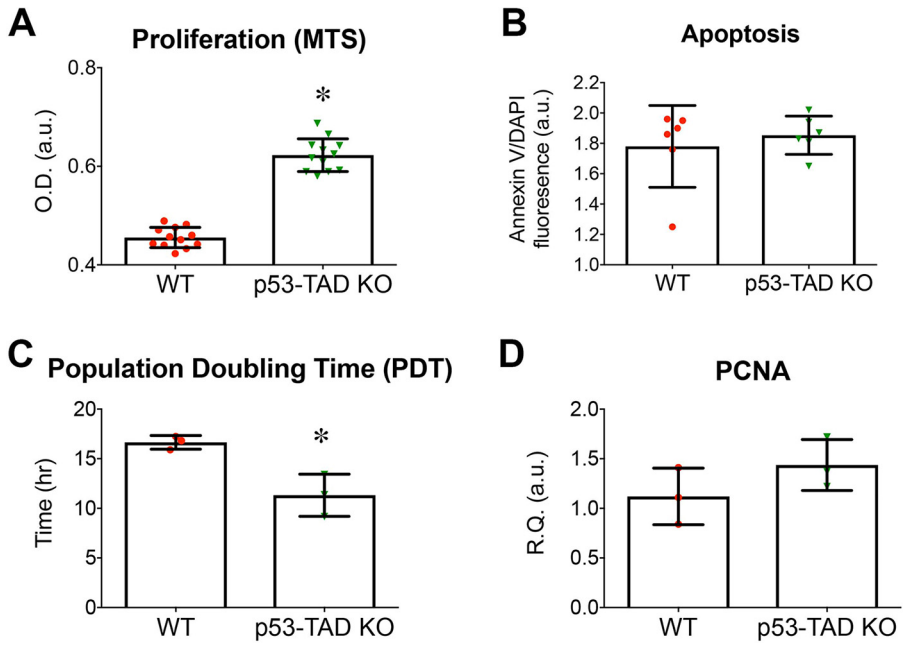

Fig. 4. p53 transactivation domain (TAD) deletion enhances the growth properties of human induced pluripotent stem cells (hiPSCs). *A* and *B*: cell proliferation (*A*) and death (*B*) measured in both wild-type (WT) and p53-TAD knockout (KO) hiPSCs. *C*: population doubling time (PDT) in WT and p53-TAD KO hiPSCs. *D*: mRNA transcript levels of proliferation cell nuclear antigen (PCNA) in both WT and p53-TAD KO hiPSCs measured by RT-PCR. Symbols denote plotted values. Data are means +/− SD; $n = 3$. *$P < 0.05$ vs. WT.

p53-TAD KO iPSCs after Doxo. Tail moment decreased dramatically in cells expressing p53-WT but remained high in cells with p53-TAD deletion after 72 h of recovery Fig. 5*F*). Importantly, after recovery, the number of γH2A.X-positive cells was found to be significantly higher in p53-TAD KO cells compared with WT-p53 iPSCs (Fig. 5*G*, H). Collectively, these data clearly indicate that deletion of p53-TAD affects the repair of DNA damage.

p53-TAD KO induces senescence in hiPSCs. Accumulation of DNA damage leads to cellular senescence (15). p53-TAD deletion leads to loss of DNA repair mechanisms. To determine whether continuous culture of p53-TAD deletion after the removal of Doxo would push the cell to permanent cell cycle arrest, both WT-p53 cells and p53-TAD cells were immunolabeled for the cellular senescence marker $p16^{INK4a}$. The fraction of $p16^{INK4a}$-positive p53-TAD cells was significantly higher compared with hiPSCs expressing WT-p53 (Fig. 6, *A* and *B*). Analysis of cell cycle using FACS revealed a significant amount of p53-TAD KO cells arrested at the G_2/M phase because of accumulation of DNA damage compared with p53-WT hiPSCs (Fig. 6, *C* and *D*). These data clearly imply that because of the loss of DNA repair processes and accumulation of damaged DNA in p53-TAD KO cells, these cells eventually become senescent by expressing the cellular senescence marker $p16^{INK4a}$.

DISCUSSION

Proper functioning of the organism is dependent on the presence of efficient mechanisms regulating the life processes of each cell within it, and, undoubtedly, p53 protein plays a primary role in regulating the multiple processes that occur, even at the organ level. p53 protects against the reproduction of cells with genome changes that result from DNA damage by stopping the cell cycle and inducing the activation of cell repair mechanisms as well as inducing cell death. In our study, we investigated the role of the TAD of p53 in DNA integrity and repair in iPSCs. For the first time, we have shown that the TAD of p53 can be deleted in hiPSCs using CRISPR/Cas9 gene KO technology and that clones of p53-TAD KO hiPSCs can be established. As a result of loss of function of p53 because of p53-TAD deletion, cells showed accelerated proliferation, a well-documented phenomenon. Western blot analysis of p53-TAD KO clones, using an antibody specific for NH_2-terminal p53, revealed an absence of p53 but reappeared when analyzed using a COOH-terminal p53 antibody. This clearly shows that the expression of other isoforms containing the p53 COOH-terminal are not affected in p53-TAD KO cells. When a domain is deleted from a protein, the remaining protein is expected to be expressed and runs as a lower molecular band in SDS-PAGE gels. With the COOH-terminal p53-specific antibody, a truncated 47-kDa p53 band was revealed in p53-TAD KO cells, which is the TAD-deleted p53 protein.

DNA damages are repaired in eukaryotes by the collaborative action of mechanisms centered on homologous recombination or nonhomologous end joining (14, 16). An extremely conserved MRN complex containing the proteins Mre11, Rad50, and Nbs1 plays critical roles in DNA damage repair (5, 29). Preceding these highly structured processes, the random broken ends of DNA needs to be identified and processed. MRN complex proteins are involved in the preliminary processing of DNA strand breaks, owing to their nuclease action and DNA-binding ability (5, 21). These events dwell in Mre11 protein and moderately depend on collaboration of Mre11 through Rad50 ATPase. The MRN complex adheres to the sites of DNA strand breaks immediately after their induction, and this process is independent of ataxia telangiectasia mutated serine/threonine kinase (ATM) (21) and precedes p53 activation (5, 21). In our analysis, Mre11 and Rad50 expression levels were unaltered in p53-TAD KO hiPSCs indicating that deletion of p53-TAD has no effect on MRN complex proteins. Chk2, a key mediator of the DNA damage response, was also activated in both cell groups after Doxo treatment (32). Similarly, histone protein H2AX, which is rapidly phosphorylated after DNA damage (25, 28) and recruited at the sites of DNA

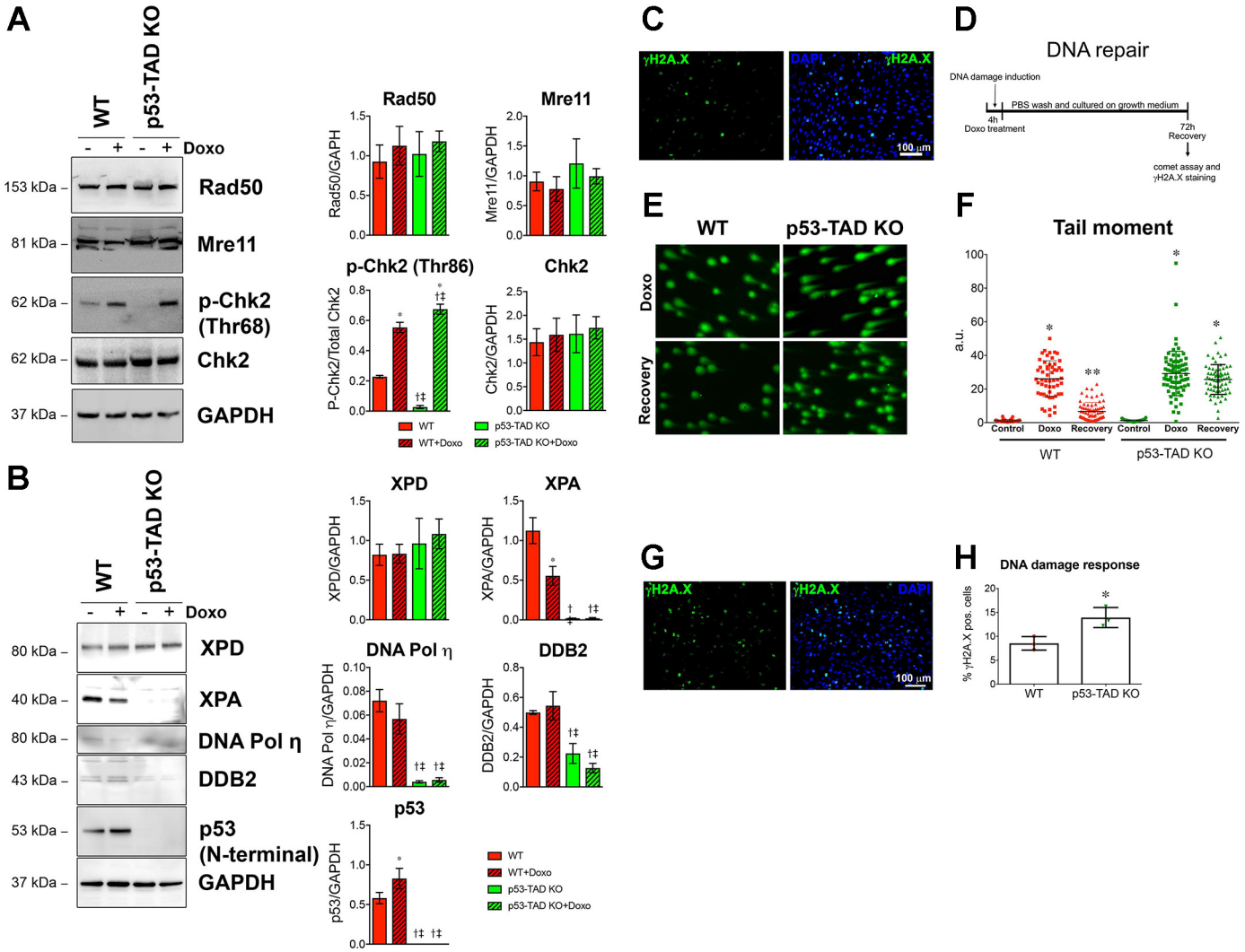

Fig. 5. p53 transactivation domain (TAD) deletion impairs DNA damage repair in human induced pluripotent stem cells (hiPSCs). *A* and *B*, *left*: Western blots of Rad50, Mre11, phosphorylated checkpoint kinase 2 (p-Chk2) at Thr^{68}, and total Chk2 (*A*) as well as xeroderma pigmentosum group D (XPD), xeroderma pigmentosum group A (XPA), DNA-binding protein 2 (DDB2), and DNA polymerase H (DNA Pol η) (*B*) in wild-type (WT) and p53-TAD knockout (KO) hiPSCs with and without doxorubicin (Doxo) treatment. Western blot quantifications are shown on the *right*. Data are means ± SD; $n = 3$ in all cases. *$P <$ 0.05 vs. the respective nontreated cells; †$P < 0.05$ vs. WT; ‡$P < 0.05$ vs. WT + Doxo. *C*: p53-TAD hiPSCs were immunolabeled for γH2A.X (green; *left*) and counterstained with DAPI (blue; *right*). *D*: schematic of DNA damage repair methodology. *E*: nucleoids in WT hiPSCs and p53-TAD KO hiPSCs treated with Doxo (*top*) and after recovery (*bottom*) were stained with Vista green dye (green). Comets were apparent with Doxo and after recovery of p53-TAD KO hiPSCs, whereas intact DNA was noted in WT hiPSCs after recovery. *F*: tail moment of WT hiPSCs and p53-TAD KO hiPSCs nuclei at baseline (control), after Doxo, and after recovery. a.u., arbitrary units. Symbols denote plotted values. Data are means ± SD; $n = 3$ in all cases. *$P < 0.05$ vs. control; **$P < 0.05$ vs. Doxo. *G*: representative micrograph of hiPSCs immunolabeled for γH2A.X (green; *left*) and nuclei stained with DAPI (blue; *right*). *H*: fraction of WT p53 and p53-TAD KO hiPSCs positive for γH2A.X. Symbols denote plotted values. Data are means ± SD; $n = 3$ in all cases. *$P < 0.05$ vs. WT.

breaks, was not affected in p53-TAD KO cells. Therefore, upstream of p53 in the DNA damage repair mechanism is not affected in p53-TAD KO iPSCs. The p53-dependant DNA repair proteins XPA and XPD play crucial roles in the nucleotide excision repair system (4). Upon p53-TAD deletion, hiPSCs lost the ability to express XPA, DNA Pol η, and DDB2 but not XPD. However, XPD expression levels did not increase in either cell group, indicating that XPD has no significant role in iPS DNA repair. Although it is very much possible that XPA may have a significant role in hiPS DNA repair, at this point it is difficult to conclude its function because a significant increase in XPA protein expression was not observed in Doxo-treated cells. Therefore, further specific gene KO studies are necessary to confirm such claims.

In our study, a milder dose of Doxo induced significant DNA damage in both WT and p53-TAD KO hiPSCs. After 72 h of recovery, only WT hiPSCs corrected their damaged DNA, whereas p53-TAD KO hiPSCs did not undergo complete DNA damage repair. This ensures the necessity of functional p53-TAD to repair damaged DNA by cells. Recently, Gong et al. (10), using a zebrafish p53 isoform Δ113p53/Δ133p53 transgenic model, showed that in response to DNA damage, p53 isoform Δ113p53/Δ133p53 promotes DNA double-strand break repair and protects cells from death and senescence. However, to our knowledge, ours is the first report to show the direct role of p53-TAD in the DNA repair process.

Functional impairment of the DNA damage mechanism both in vitro (19) and in vivo (17) leads to an accumulation of

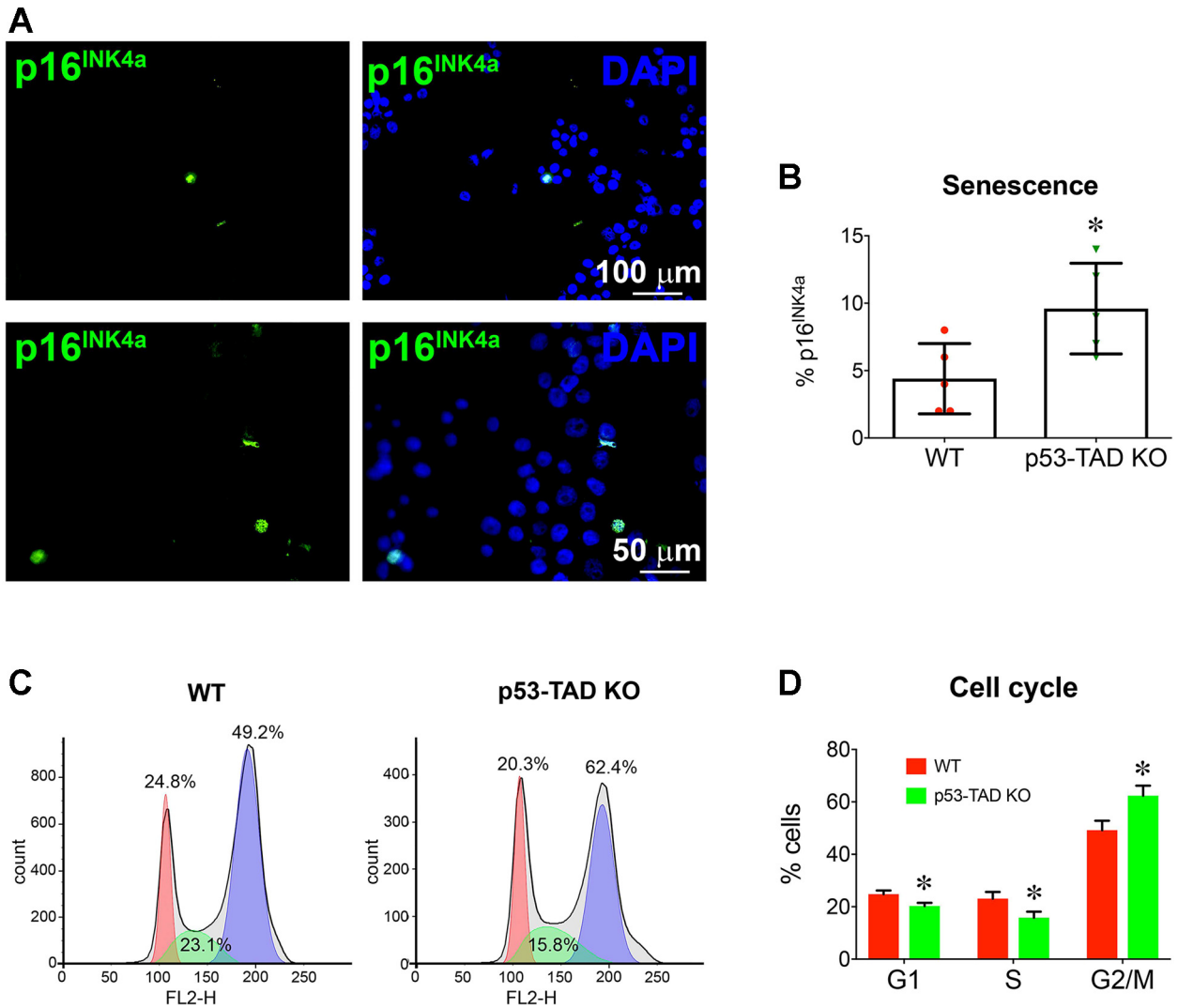

Fig. 6. p53 transactivation domain (TAD) deletion affects the senescence of human induced pluripotent stem cells (hiPSCs). *A*: representative micrographs of p53-TAD knockout (KO) hiPSCs immunolabeled for $p16^{INK4a}$ (green); nuclei were stained with DAPI (blue). *B*: fraction of wild-type (WT) and p53-TAD KO hiPSCs positive for $p16^{INK4a}$. *C*: cell cycle arrest as analyzed by FACS. *D*: fraction of WT hiPSCs and p53-TAD KO hiPSCs in G_1, S, and G_2/M cell cycle phases. Data are means ± SD. $^*P < 0.05$ vs. WT.

damaged DNA, which induces premature aging and expression of the cellular senescent marker $p16^{INK4a}$ (2). In agreement with a previous finding (19), we also observed that prolonged, continuous culture of p53-TAD hiPSCs arrest at G_2/M, express $p16^{INK4a}$, and become senescent. The role of p53-TAD in the accumulation of DNA damage induced cellular aging in hiPSCs has never been reported. Here, we clearly show that p53-TAD deletion in hiPSCs leads to DNA damage accumulation and drives the cells to cellular senescence. Because both TADs were deleted in p53-TAD KO hiPSCs, the findings that *1*) the necessity of p53-TAD for DNA repair and integrity and *2*) p53-TAD prevents cellular senescence should be attributed to both TAD1 and TAD2. However, given the role of TAD1 in apoptosis, we can speculate that TAD2 alone is responsible for the above-stated functions. In any case, to distinguish the roles of TAD1 and TAD2 on DNA repair, further studies are warranted.

Recently, Nakada et al. (22) demonstrated that a hypoxic regime reduces mitochondrial metabolism and promotes proliferation in cardiomyocytes, resulting in increased regeneration after myocardial infarction in mouse models. Furthermore, the report showed that systemic hypoxemia in mice resulted in inhibition of oxidative metabolism, decreased production of reactive oxygen species and oxidative DNA damage, and reactivation of cardiomyocyte mitosis (22). Therefore, preventing oxidative DNA damage or promoting DNA damage repair has great potential in cardiac regeneration. However, the induction of prolonged hypoxia is poorly tolerated (22), and organ/cell type-specific hypoxia induction in mammalians is merely impossible. Here, we showed that p53-TAD plays a crucial role in DNA repair and integrity. Small molecules that can selectively activate p53-TAD to promote DNA repair and integrity can be designed and developed to overcome this critical clinical issue.

Conclusions. iPSCs and iPS-derived cells have immense potential in regenerative medicine, including cardiac regeneration (24). Reprogramming-induced genome instability in iPSCs causes tumor formation in vivo (1). This major clinical issue complicates the use of iPS-derived cells to regenerate the

injured myocardium. Our findings clearly show that p53-TAD is required for the cells to retain DNA integrity, and, to our knowledge, this is the first report showing the direct role of p53-TAD on DNA repair mechanisms. Small molecule-based p53-TAD activators could promote DNA integrity in iPSCs and iPS-derived cells. Before cell transplantation, for the purpose of cardiac regeneration, cells can be treated to promote DNA integrity and prevent tumor formation by transplanted cells.

GRANTS

This work was supported in part by National Heart, Lung, and Blood Institute Grants RO1-HL-99507, HL-114120, HL-131017, HL-138023, and UO1-HL-134764 (to J. Zhang) and by American Heart Association Scientific Development Grant 17SDG33670677 (to R. Kannappan).

DISCLOSURES

No conflicts of interest, financial or otherwise, are declared by the authors.

AUTHOR CONTRIBUTIONS

R.K. and S.M. conceived and designed research; R.K., S.M., and P.A.W. performed experiments; R.K. and S.M. analyzed data; R.K., S.M., P.A.W., and J.Z. interpreted results of experiments; R.K. and S.M. prepared figures; R.K. drafted manuscript; R.K. edited and revised manuscript; R.K., S.M., P.A.W., and J.Z. approved final version of manuscript.

REFERENCES

1. **Bai Q, Desprat R, Klein B, Lemaître JM, De Vos J.** Embryonic stem cells or induced pluripotent stem cells? A DNA integrity perspective. *Curr Gene Ther* 13: 93–98, 2013. doi:10.2174/1566523211313020003.
2. **Chen JH, Hales CN, Ozanne SE.** DNA damage, cellular senescence and organismal ageing: causal or correlative? *Nucleic Acids Res* 35: 7417–7428, 2007. doi:10.1093/nar/gkm681.
3. **Chène P.** The role of tetramerization in p53 function. *Oncogene* 20: 2611–2617, 2001. doi:10.1038/sj.onc.1204373.
4. **Chiang CC, Tsai YY, Bau DT, Cheng YW, Tseng SH, Wang RF, Tsai FJ.** Pterygium and genetic polymorphisms of the DNA repair enzymes XRCC1, XPA, and XPD. *Mol Vis* 16: 698–704, 2010.
5. **D'Amours D, Jackson SP.** The Mre11 complex: at the crossroads of dna repair and checkpoint signalling. *Nat Rev Mol Cell Biol* 3: 317–327, 2002. doi:10.1038/nrm805.
6. **Dawson R, Müller L, Dehner A, Klein C, Kessler H, Buchner J.** The N-terminal domain of p53 is natively unfolded. *J Mol Biol* 332: 1131–1141, 2003. doi:10.1016/j.jmb.2003.08.008.
7. **El-Deiry WS.** The role of p53 in chemosensitivity and radiosensitivity. *Oncogene* 22: 7486–7495, 2003. doi:10.1038/sj.onc.1206949.
8. **Evan GI, Brown L, Whyte M, Harrington E.** Apoptosis and the cell cycle. *Curr Opin Cell Biol* 7: 825–834, 1995. doi:10.1016/0955-0674(95)80066-2.
9. **Fennema M, Erdmann W, Faithfull NS.** Myocardial oxygen supply under critical conditions, the effects of hemodilution and fluorocarbons. *Adv Exp Med Biol* 317: 527–544, 1992. doi:10.1007/978-1-4615-3428-0_63.
10. **Gong L, Gong H, Pan X, Chang C, Ou Z, Ye S, Yin L, Yang L, Tao T, Zhang Z, Liu C, Lane DP, Peng J, Chen J.** p53 isoform Δ113p53/Δ133p53 promotes DNA double-strand break repair to protect cell from death and senescence in response to DNA damage. *Cell Res* 25: 351–369, 2015. doi:10.1038/cr.2015.22.
11. **Hamard PJ, Lukin DJ, Manfredi JJ.** p53 basic C terminus regulates p53 functions through DNA binding modulation of subset of target genes. *J Biol Chem* 287: 22397–22407, 2012. doi:10.1074/jbc.M111.331298.
12. **Harms KL, Chen X.** The functional domains in p53 family proteins exhibit both common and distinct properties. *Cell Death Differ* 13: 890–897, 2006. doi:10.1038/sj.cdd.4401904.
13. **Hirakawa K, Midorikawa K, Oikawa S, Kawanishi S.** Carcinogenic semicarbazide induces sequence-specific DNA damage through the generation of reactive oxygen species and the derived organic radicals. *Mutat Res* 536: 91–101, 2003. doi:10.1016/S1383-5718(03)00030-5.
14. **Hopfner KP, Putnam CD, Tainer JA.** DNA double-strand break repair from head to tail. *Curr Opin Struct Biol* 12: 115–122, 2002. doi:10.1016/S0959-440X(02)00297-X.
15. **Itahana K, Dimri G, Campisi J.** Regulation of cellular senescence by p53. *Eur J Biochem* 268: 2784–2791, 2001. doi:10.1046/j.1432-1327.2001.02228.x.
16. **Jackson SP.** Sensing and repairing DNA double-strand breaks. *Carcinogenesis* 23: 687–696, 2002. doi:10.1093/carcin/23.5.687.
17. **Lombard DB, Chua KF, Mostoslavsky R, Franco S, Gostissa M, Alt FW.** DNA repair, genome stability, and aging. *Cell* 120: 497–512, 2005. doi:10.1016/j.cell.2005.01.028.
18. **Lorenzo Y, Costa S, Collins AR, Azqueta A.** The comet assay, DNA damage, DNA repair and cytotoxicity: hedgehogs are not always dead. *Mutagenesis* 28: 427–432, 2013. doi:10.1093/mutage/get018.
19. **Lou Z, Chen J.** Cellular senescence and DNA repair. *Exp Cell Res* 312: 2641–2646, 2006. doi:10.1016/j.yexcr.2006.06.009.
20. **Martinez GR, Loureiro AP, Marques SA, Miyamoto S, Yamaguchi LF, Onuki J, Almeida EA, Garcia CC, Barbosa LF, Medeiros MH, Di Mascio P.** Oxidative and alkylating damage in DNA. *Mutat Res* 544: 115–127, 2003. doi:10.1016/j.mrrev.2003.05.005.
21. **Mirzoeva OK, Petrini JH.** DNA damage-dependent nuclear dynamics of the Mre11 complex. *Mol Cell Biol* 21: 281–288, 2001. doi:10.1128/MCB.21.1.281-288.2001.
22. **Nakada Y, Canseco DC, Thet S, Abdisalaam S, Asaithamby A, Santos CX, Shah AM, Zhang H, Faber JE, Kinter MT, Szweda LI, Xing C, Hu Z, Deberardinis RJ, Schiattarella G, Hill JA, Oz O, Lu Z, Zhang CC, Kimura W, Sadek HA.** Hypoxia induces heart regeneration in adult mice. *Nature* 541: 222–227, 2017. doi:10.1038/nature20173.
23. **Napoli M, Flores ER.** The p53 family orchestrates the regulation of metabolism: physiological regulation and implications for cancer therapy. *Br J Cancer* 116: 149–155, 2017. doi:10.1038/bjc.2016.384.
24. **Okita K, Yamanaka S.** Induced pluripotent stem cells: opportunities and challenges. *Philos Trans R Soc Lond B Biol Sci* 366: 2198–2207, 2011. doi:10.1098/rstb.2011.0016.
25. **Paull TT, Rogakou EP, Yamazaki V, Kirchgessner CU, Gellert M, Bonner WM.** A critical role for histone H2AX in recruitment of repair factors to nuclear foci after DNA damage. *Curr Biol* 10: 886–895, 2000. doi:10.1016/S0960-9822(00)00610-2.
26. **Raj N, Attardi LD.** The transactivation domains of the p53 protein. *Cold Spring Harb Perspect Med* 7: a026047, 2017. doi:10.1101/cshperspect.a026047.
27. **Riley T, Sontag E, Chen P, Levine A.** Transcriptional control of human p53-regulated genes. *Nat Rev Mol Cell Biol* 9: 402–412, 2008. doi:10.1038/nrm2395.
28. **Rogakou EP, Pilch DR, Orr AH, Ivanova VS, Bonner WM.** DNA double-stranded breaks induce histone H2AX phosphorylation on serine 139. *J Biol Chem* 273: 5858–5868, 1998. doi:10.1074/jbc.273.10.5858.
29. **Tauchi H, Kobayashi J, Morishima K, van Gent DC, Shiraishi T, Verkaik NS, vanHeems D, Ito E, Nakamura A, Sonoda E, Takata M, Takeda S, Matsuura S, Komatsu K.** Nbs1 is essential for DNA repair by homologous recombination in higher vertebrate cells. *Nature* 420: 93–98, 2002. doi:10.1038/nature01125.
30. **Valko M, Rhodes CJ, Moncol J, Izakovic M, Mazur M.** Free radicals, metals and antioxidants in oxidative stress-induced cancer. *Chem Biol Interact* 160: 1–40, 2006. doi:10.1016/j.cbi.2005.12.009.
31. **Wiseman H, Halliwell B.** Damage to DNA by reactive oxygen and nitrogen species: role in inflammatory disease and progression to cancer. *Biochem J* 313: 17–29, 1996. doi:10.1042/bj3130017.
32. **Zannini L, Delia D, Buscemi G.** CHK2 kinase in the DNA damage response and beyond. *J Mol Cell Biol* 6: 442–457, 2014. doi:10.1093/jmcb/mju045.
33. **Zhang L, Guo J, Zhang P, Xiong Q, Wu SC, Xia L, Roy SS, Tolar J, O'Connell TD, Kyba M, Liao K, Zhang J.** Derivation and high engraftment of patient-specific cardiomyocyte sheet using induced pluripotent stem cells generated from adult cardiac fibroblast. *Circ Heart Fail* 8: 156–166, 2015. doi:10.1161/CIRCHEARTFAILURE.114.001317.
34. **Zhang X, Cheng Q, Yin H, Yang G.** Regulation of autophagy and EMT by the interplay between p53 and RAS during cancer progression (review) [Review]. *Int J Oncol* 51: 18–24, 2017. doi:10.3892/ijo.2017.4025.
35. **Zhu J, Zhang S, Jiang J, Chen X.** Definition of the p53 functional domains necessary for inducing apoptosis. *J Biol Chem* 275: 39927–39934, 2000. doi:10.1074/jbc.M005676200.
36. **Zhu J, Zhou W, Jiang J, Chen X.** Identification of a novel p53 functional domain that is necessary for mediating apoptosis. *J Biol Chem* 273: 13030–13036, 1998. doi:10.1074/jbc.273.21.13030.